CHEMISTRY
A EUROPEAN JOURNAL

ChemPubSoc
Europe

DOI: 10.1002/chem.201202657

Am(m)ines Make the Difference: Organoruthenium Am(m)ine Complexes and Their Chemistry in Anticancer Drug Development

Maria V. Babak,[a] Samuel M. Meier,[a, b] Anton A. Legin,[a] Mahsa S. Adib Razavi,[a] Alexander Roller,[a] Michael A. Jakupec,[a, b] Bernhard K. Keppler,[a, b] and Christian G. Hartinger *[a, b, c]

Abstract: With the aim of systematically studying fundamental structure–activity relationships as a basis for the development of Ru^{II} arene complexes (arene = *p*-cymene or biphenyl) bearing mono-, bi-, or tridentate am(m)ine ligands as anticancer agents, a series of ammine, ethylenediamine, and diethylenetriamine complexes were prepared by different synthetic routes. Especially the synthesis of mono-, di-, and triammine complexes was found to be highly dependent on the reaction conditions, such as stoichiometry, temperature, and time. Hydrolysis and protein-binding studies were performed to determine the reactivity of the compounds, and only those containing chlorido ligands undergo aquation or form protein adducts. These properties correlate well with in vitro tumor-inhibiting potency of the compounds. The complexes were found to be active in anticancer assays when meeting the following criteria: stability in aqueous solution and low rates of hydrolysis and binding to proteins. Therefore, the complexes least reactive to proteins were found to be the most cytotoxic in cancer cells. In general, complexes with biphenyl as arene ligand inhibited the growth of tumor cells more effectively than the cymene analogues, consistent with the increase in lipophilicity. This study highlights the importance of finding a proper balance between reactivity and stability in the development of organometallic anticancer agents.

Keywords: arene ligands · cancer · N ligands · ruthenium · structure–activity relationships

Introduction

The discovery of the anticancer activity of cisplatin by Rosenberg et al.[1] has broadened the range of routinely applied chemotherapeutics from organic drugs to metal-based compounds. Complexes based on titanium,[2] arsenic, and ruthenium[2a,3] succeeded cisplatin in clinical trials, and especially Ru anticancer agents show promising results.[4] The unique properties of Ru compounds are thought to be related to an enhanced degree of selectivity compared to many other metallodrugs due to binding to proteins in the blood stream and activation by reduction ($Ru^{III/II}$) once inside the tumor.[4b,5] As cisplatin consists of a Pt^{II} core with two ammine and two chlorido ligands, researchers focused initially on analogous multichlorido ruthenium complexes with ammine ligands. Two mixed-valent ruthenium complexes, namely, $[(NH_3)_5Ru^{III}ORu^{IV}(NH_3)_4ORu^{III}(NH_3)_5]^{6+}$ (ruthenium red) and $[Cl(NH_3)_4Ru^{III}ORu^{IV}(NH_3)_4(OH)]^{3+}$ (Ru360), which have been used as cytological stains,[6] were found to be inhibitors of the mitochondrial uniporter (Ca^{2+} uptake)[7] and, like other ruthenium compounds, such as $[Ru^{III}(py)(NH_3)_5]^{3+}$ (py = pyridine), *cis*-$[Ru^{III}(Him)_2(NH_3)_4]$ (Him = imidazole), they show remarkable immunosuppressant activity.[3a,8] The extensive work of Clarke and colleagues demonstrated that am(m)ine coordination complexes of Ru^{III} and Ru^{II} are active antitumor agents (e.g., *cis*-$[Ru^{III}Cl_2(NH_3)_4]^+$,[9] *fac*-$[Ru^{III}Cl_3(NH_3)_3]$,[10] $[Ru^{III}(O_2CCH_2CH_3)(NH_3)_5]^{2+}$,[3a] $[Ru^{II}(H_2O)(NH_3)_5]^{2+}$,[11] etc.).[3a,12] Other studies indicated the potential of mixed-ligand ruthenium(II) complexes with ethylenediamine and its derivatives.[13] In contrast to cisplatin, which is known to form preferably intrastrand cross-links between adjacent guanine residues of DNA,[14] ruthenium am(m)ine complexes favor interstrand cross-link formation, probably due to the steric hindrance of the octahedrally configured ruthenium center as opposed to the less crowded square-planar coordination geometry of Pt^{II}.[3a] Although the complexes exhibited very good anticancer activity in primary tumors, low solubility prevented

[a] M. V. Babak, S. M. Meier, A. A. Legin, M. S. Adib Razavi, A. Roller, Dr. M. A. Jakupec, Prof. Dr. B. K. Keppler, Prof. Dr. C. G. Hartinger
Institute of Inorganic Chemistry
University of Vienna
Waehringer Strasse 42, 1090 Vienna (Austria)

[b] S. M. Meier, Dr. M. A. Jakupec, Prof. Dr. B. K. Keppler, Prof. Dr. C. G. Hartinger
Research Platform "Translational Cancer Therapy Research"
University of Vienna
Waehringer Strasse 42, 1090 Vienna (Austria)

[c] Prof. Dr. C. G. Hartinger
School of Chemical Sciences
The University of Auckland
Private Bag 92019, Auckland 1142 (New Zealand)
Fax: (+64) 9-3737-599 ext. 87422
E-mail: c.hartinger@auckland.ac.nz

Supporting information for this article is available on the WWW under http://dx.doi.org/10.1002/chem.201202657.

their further development. However, complexes with simple nitrogen-containing ligands (NH_3, 1,2-ethylenediamine, pyridine) other than indazole and imidazole proved to have potential in anticancer drug development.

More recently, Ru^{II} arene compounds made an appearance in medicinal chemistry, and their biological activity is significantly dependent on the nature of the coligands.[3b,15] Complexes of the type $[(\eta^6\text{-arene})Ru(en)X]^+$ with bidentate ethylenediamine (en) and chloride as a leaving group (X) exhibited excellent cytotoxicity against primary tumors which was in good correlation with their DNA binding ability.[16] Surprisingly, recently published neutral half-sandwich ruthenium complexes $[(\eta^6\text{-arene})Ru(NH_3)Cl_2]$ (arene = *p*-cymene or biphenyl) do not inhibit the growth of tumor cells in an in vitro setting, probably due to their low aqueous stability and high reactivity in cell culture medium.[17] Similar observations were also made with other Ru(arene) complexes, the cytotoxicity of which greatly depends on their reactivity.[18] To control interactions with the wide variety of biomolecules present in the cell, the choice of the type of ligands (chelating/nonchelating), arene (more/less lipophilic), and the presence of a leaving group (inert/labile to aquation as an activation step) is of high importance. With the aim of weaving together all of the disparate threads running through the development of half-sandwich Ru^{II} complexes bearing various am(m)ine ligands, we present a systematic investigation including their synthesis, spectroscopic properties, crystal structures, behavior in aqueous solution, and studies on their antiproliferative activity in cancer cells and interactions with biomolecules.

Experimental Section

Materials and methods: Materials from chemical suppliers were used as received, and all reactions were carried out under argon atmosphere in anhydrous solvents if not otherwise stated. $RuCl_3 \cdot 3H_2O$ was purchased from Johnson Matthey. $[(\eta^6\text{-}p\text{-cymene})Ru^{II}(\text{ethylenediamine})Cl]PF_6$ (**7a**), $[(\eta^6\text{-biphenyl})Ru^{II}(\text{ethylenediamine})Cl]PF_6$ (**7b**),[19] $[\{(\eta^6\text{-}p\text{-cymene})RuCl_2\}_2]$ (**A**), and $[\{(\eta^6\text{-biphenyl})RuCl_2\}_2]$ (**B**)[20] were prepared according to literature procedures. Methanol was dried and distilled over Mg under argon atmosphere. Ethylenediamine was distilled over Na prior to use or was purchased from Aldrich (purified by redistillation, >99.5%). NH_4OH (25% solution in water) and formic acid (98%) were obtained from Fluka; NH_4PF_6 (>95%), $AgPF_6$ (98%), diethylenetriamine (97%) from Aldrich; and ubiquitin (from bovine erythrocytes) and horse heart cytochrome c from Sigma. Dimethyl sulfoxide was obtained from Acros, and 9-ethylguanine (EtG) from Sigma. Products were isolated without taking any special precautions, but anhydrous solvents were used for isolation of **2a**, **2b**, **5a**, **5b**, **6a**, **7a**, and **7b**.

Elemental analyses were performed by the Microanalytical Laboratory of the Faculty of Chemistry of the University of Vienna. Electrospray ionization mass spectrometry was carried out with a Bruker Esquire 3000 instrument (Bruker Daltonics, Bremen, Germany), MilliQ water (18.2 MΩ; Millipore Synergy 185 UV Ultrapure Water System; Molsheim, France) and methanol (VWR Int., HiPerSolv, CHROMANORM) were used as solvents for ESI-MS studies. The ^1H and ^{31}P NMR spectra were recorded at 500.10 and 202.44 MHz on a Bruker FT NMR spectrometer Avance II 500 MHz. ^1H NMR kinetic experiments were performed at 500.32 MHz on a Bruker DPX500 (Ultrashield Magnet). Chemical shifts are given in parts per million (ppm) relative to the residual solvent peak. NaOD (40% in D_2O, Fluka) was used for H/D-exchange NMR experiments.

X-ray diffraction measurements were performed on a Bruker X8 APEX II CCD diffractometer at 100 (**2b**, **6a**), 150 (**4b**), or 296 K (**3a**). Single crystals were positioned 40, 35, 35, and 35 mm from the detector, and 1468, 2295, 2780 and 823 frames were measured, each for 10, 30, 10 and 10 s over 1° scan width for **2b**, **3a**, **4b**, and **6a**, respectively. The data were processed with SAINT software.[21] Crystal data, data collection parameters, and structure refinement details for **2b**, **3a**, **4b**, and **6a** are given in Table S1 of the Supporting Information and key bond lengths and angles in Table S2. The structures were solved by direct methods and refined by full-matrix least-squares techniques. Non-hydrogen atoms were refined with anisotropic displacement parameters. Hydrogen atoms were placed at calculated positions and refined as riding atoms in the subsequent least squares model refinements. The isotropic thermal parameters were estimated to be 1.2 times the values of the equivalent isotropic thermal parameters of the non-hydrogen atoms to which hydrogen atoms are bonded. Severe disorder of the hexafluorophosphate anion in **3a**, modeled with two positions for P1, resulted in relatively high residual electron density. The following computer programs, equipment and tables were used: structure solution, SHELXS-97; refinement, SHELXL-97;[22] molecular diagrams, Mercury 3.0.

Cell lines and culture conditions: The human cancer cell line CH1 (ovarian carcinoma) was provided by Lloyd R. Kelland (CRC Centre for Cancer Therapeutics, Institute of Cancer Research, Sutton, UK). A549 (non-small cell lung cancer) and SW480 (colon carcinoma) cells were supplied by Brigitte Marian (Institute of Cancer Research, Department of Medicine I, Medical University of Vienna, Austria). Adherent cell cultures were grown in 75 cm^2 culture flasks (Iwaki/Asahi Technoglass, Gyouda, Japan) in complete medium [i.e., minimal essential medium (MEM) supplemented with 10% heat-inactivated fetal bovine serum, 1 mM sodium pyruvate, 4 mM L-glutamine, and 1% v/v nonessential amino acids from 100× ready-to-use stock (all purchased from Sigma-Aldrich, Austria)]. Cell cultures were incubated at 37°C in a moist atmosphere containing 5% CO_2.

Cytotoxicity test in cancer cell lines: The cytotoxicity of the compounds was determined by means of a colorimetric microculture assay (MTT assay). The cells were harvested from culture flasks by trypsinization and seeded into 96-well microculture plates (Iwaki/Asahi Technoglass, Gyouda, Japan) in densities of 1×10^3 cells per well (for CH1), 2.5×10^3 cells per well (for SW480), and 3×10^3 cells per well (for A549). After the cells were allowed to resume exponential growth for 24 h, the test compounds were dissolved in complete medium and 100 μL of serial dilution was added per well. After exposure for 96 h, drug solutions were replaced with 100 μL of RPMI 1640 culture medium (supplemented with 10% heat-inactivated fetal bovine serum and 2 mM of L-glutamine) plus 20 μL of MTT solution in phosphate-buffered saline (5 mg mL^{-1}). After incubation for 4 h, the RPMI/MTT mixtures were removed, and the formazan crystals formed in viable cells were dissolved in 150 μL of DMSO per well. Optical densities were measured at 550 nm with a microplate reader (Tecan Spectra Classic), by using a reference wavelength of 690 nm to correct for unspecific absorption. The quantity of viable cells was expressed in terms of treated/control (T/C) values by comparison to untreated control microcultures, and 50% inhibitory concentrations (IC_{50}) were calculated from concentration–effect curves by interpolation. Evaluation was based on means from at least three independent experiments, each comprising three replicates per concentration level.

Protein-binding studies: The metal compounds (400 μM) were dissolved in 1% aqueous dimethyl sulfoxide, and the proteins ubiquitin and cytochrome c (200 μM) in water. These stock solutions were mixed to obtain 2:1 metal-to-protein molar ratios and then kept at 37°C in the dark. Mass spectra of the incubation solutions were recorded after 0, 3, 6, 24, and 48 h. Furthermore, the compounds were incubated under comparable conditions with an ubiquitin–cytochrome c mixture to yield a molar ratio of 1:1:1.

The samples were analyzed by using a MaXis ESI-Q-ToF mass spectrometer (Bruker Daltonics, Bremen, Germany) with the following parameters: capillary −4.5 kV, gas flow 8 psi, dry gas 6 L min^{-1}, dry temperature

150 °C, 400 V_{pp} funnel RF, 4 eV quadrupole ion energy and 100 μs transfer time. The samples were diluted to 2 μM with water/methanol/formic acid (50:50:0.2) and thereafter injected into the mass spectrometer by direct infusion at a flow rate of 180 μL h^{-1}. The spectra were recorded in positive-ion mode over 0.5 min and averaged. The Data Analysis 4.0 software package (Bruker Daltonics, Bremen, Germany) was used for processing, and maximum entropy deconvolution (automatic data point spacing and 30000 instrument resolving power) was applied.

Binding to the DNA model 9-ethylguanine: Compounds **2b**, **5b**, and **7b** (400 μM) were dissolved in 1% dimethyl sulfoxide aqueous solution. EtG (800 μM) was dissolved in water. The compounds and EtG were incubated at 1:2 molar ratio at metal-to-complex concentrations of 50–100 μM for 3, 6, 24, and 48 h at 37 °C. Samples were diluted with water/methanol (1:1) to final concentrations of 5–10 μM and immediately introduced into the mass spectrometer. ESI-IT mass spectra were recorded on an AmaZon Ion Trap mass spectrometer (Bruker Daltonics, Bremen Germany) by direct infusion at a flow rate of 180 μL h^{-1}. The following parameters were employed: capillary −2.5 kV, gas flow 9 psi, dry gas 6 L min^{-1}, dry temperature 200 °C, and trap drive 55.1. The Data Analysis 4.0 software package (Bruker Daltonics, Bremen, Germany) was used for processing the raw data.

Synthesis of complexes

*[(η^6-p-cymene)$Ru^{II}(NH_3)_3$]$(PF_6)_2$ (**1a**)*: Method 1: [{(η^6-*p*-cymene)$RuCl_2$}$_2$] (0.3 mmol, 0.184 g) was stirred for 10 min in dry methanol (10 mL). Ammonia gas was bubbled through the solution, which caused significant warming of the reaction mixture and was accompanied by a fast change of the color from red-orange to light yellow. After the solution had cooled down, the gas supply was stopped and the reaction mixture was stirred for 30 min. The yellow solution was concentrated by rotary evaporation under reduced pressure to 1 mL, and a saturated solution of NH_4PF_6 in methanol (2–4 mL) was added. The resulting solution was filtered and diethyl ether (15 mL) added. The light yellow precipitate was collected by filtration, washed with diethyl ether (3×5 mL), and dried in vacuo to yield 286 mg (90%) of the target complex.

Method 2: Ammonia (2 mL, 25% aqueous solution) was added to a suspension of [{(η^6-*p*-cymene)$RuCl_2$}$_2$] (0.2 mmol, 0.122 g) in dry methanol (10 mL). The reaction mixture was heated to reflux for 1 h at 85 °C. The resulting yellow solution was concentrated by rotary evaporation under reduced pressure to 1 mL and a saturated solution of NH_4PF_6 in methanol (2–4 mL) was added. The resulting solution was filtered and diethyl ether (15 mL) was added. The yellow precipitate was collected by filtration, washed with diethyl ether (3×5 mL), and dried in vacuo to yield 152 mg (64%) of the target complex.

Elemental analysis (%) calcd for $C_{10}H_{23}RuN_3P_2F_{12}\cdot 0.1\,NH_4PF_6$ (592.61 g mol^{-1}): C 20.26, H 3.98, N 7.33; found: C 20.01, H 3.82, N 7.23%; MS (ESI+): *m/z* 270.1 {[(η^6-*p*-cymene)$Ru(NH_3)_2$−H]$^+$+[(η^6-*p*-cymene)$Ru(NH_3)_2$]$^+$}; found: 270.0; MS (ESI−): *m/z* 145.0 $[PF_6]^-$; found: 144.5; ^{1}H NMR (500.10 MHz, [D$_6$]DMSO): δ = 1.19 (d, 6H, $^3J_{HH}$ = 7.0 Hz, CH(CH_3)$_2$), 2.12 (s, 3H, C_6H_4(CH_3)), 2.81 (sept, 1H, $^3J_{HH}$ = 6.9 Hz, C*H*Me$_2$), 3.41 (s, 9H, NH_3), 5.41 (d, 2H, $^3J_{HH}$ = 6.0 Hz, CH_{cym}), 5.70 ppm (d, 2H, $^3J_{HH}$ = 6.0 Hz, CH_{cym}); ^{31}P NMR (202.44 MHz; [D$_6$]DMSO): δ = −144.10 ppm (sept, 1P, $^1J_{PF}$ = 727.7 Hz, PF_6).

*[(η^6-biphenyl)$Ru^{II}(NH_3)_3$]$(PF_6)_2$ (**1b**)*: Method 1: [{(η^6-biphenyl)$RuCl_2$}$_2$] (0.2 mmol, 0.130 g) was stirred for 10 min in dry methanol (10 mL). Ammonia gas was bubbled through the solution, which caused significant warming of the reaction mixture and changed the black-brown suspension to a light yellow solution. After the solution had cooled, the gas supply was stopped and the reaction mixture was stirred for 1 h. The yellow solution was filtered and concentrated by rotary evaporation under reduced pressure to 1 mL, and saturated solution of NH_4PF_6 in water (2–4 mL) was added. A light yellow precipitate formed immediately, which was collected by filtration, washed with water (2×2 mL) and diethyl ether (3×15 mL), and dried in vacuo to yield 175 mg (70%) of the target complex.

Method 2: Ammonia (2 mL of 25% aqueous solution) was added to a suspension of [{(η^6-biphenyl)$RuCl_2$}$_2$] (0.2 mmol, 0.130 g) in dry methanol (15 mL) and the reaction mixture was heated to reflux for 1 h at 85 °C. Then it was filtered, the resulting light-orange solution concentrated by rotary evaporation under reduced pressure to 1 mL, and a saturated solution of NH_4PF_6 in water (2–4 mL) added. The orange-yellow precipitate was collected by filtration, washed with water (1×2 mL) and diethyl ether (3×15 mL), and dried in vacuo to give 160 mg (64%) of the target product.

Elemental analysis (%) calcd for $C_{12}H_{19}RuN_3P_2F_{12}\cdot 0.2\,NH_4PF_6$ (628.90 g mol^{-1}): C 22.92, H 3.17, N 7.13; found: C 22.77, H 3.24, N 6.86%; MS (ESI+): *m/z* 290.0 {[(η^6-biphenyl)$Ru(NH_3)_2$−H]$^+$+[(η^6-biphenyl)$Ru(NH_3)_2$]$^+$}; found: 290.0; MS (ESI−): *m/z* 145.0 $[PF_6]^-$; found: 144.5; ^{1}H NMR (500.10 MHz; [D$_6$]DMSO): δ = 3.51 (s, 9H, NH_3), 5.87 (m, 3H, CH_{phen}), 6.17 (m, 2H, CH_{phen}), 7.57 (m, 3H, $RuCH_{phen}$), 7.78 ppm (m, 2H, $RuCH_{phen}$); ^{31}P NMR (202.44 MHz; [D$_6$]DMSO): δ = −144.13 ppm (sept, 1P, $^1J_{PF}$ = 720.5 Hz, PF_6).

*[(η^6-p-cymene)$Ru^{II}(NH_3)_2Cl$]PF_6 (**2a**)*: Ammonia (150 μL of 25% aqueous solution) was added to a suspension of [{(η^6-*p*-cymene)$RuCl_2$}$_2$] (0.2 mmol, 0.122 g) in dry methanol (10 mL) and the reaction mixture was heated to reflux for 1 h at 85 °C. The resulting orange solution was concentrated by rotary evaporation under reduced pressure to 1 mL and a saturated solution of NH_4PF_6 in methanol (2–4 mL) was added. The resulting bright orange solution was filtered and diethyl ether (15 mL) was added. The yellow precipitate was collected by filtration, washed with diethyl ether (3×5 mL) and dried in vacuo to yield 88 mg (49%) of the target complex.

Elemental analysis (%) calcd for $C_{10}H_{20}RuN_2PF_6Cl$ (449.77 g mol^{-1}): C 26.70, H 4.48, N 6.23, found: C 26.68, H 4.33, N 6.04%; MS (ESI+): *m/z* 288.0 [(η^6-*p*-cymene)$Ru(NH_3)Cl$]$^+$; found: 288.4; MS (ESI−): *m/z* 145.0 $[PF_6]^-$; found: 144.9; ^{1}H NMR (500.10 MHz; [D$_6$]DMSO): δ = 1.21 (d, $^3J_{HH}$ = 7.0 Hz, 6H, CH(CH_3)$_2$), 2.12 (s, 3H, C_6H_4(CH_3)), 2.81 (sept, 1H, $^3J_{HH}$ = 6.9 Hz, C*H*Me$_2$), 3.37 (s, 6H, NH_3), 5.37 (d, 2H, $^3J_{HH}$ = 6.0 Hz, CH_{cym}), 5.61 ppm (d, 2H, $^3J_{HH}$ = 6.1 Hz, CH_{cym}); ^{31}P NMR (202.44 MHz; [D$_6$]DMSO): δ = −144.15 ppm (sept, 1P, $^1J_{PF}$ = 702.7 Hz, PF_6).

*[(η^6-biphenyl)$Ru^{II}(NH_3)_2Cl$]PF_6 (**2b**)*: Ammonia (150 μL of 25% aqueous solution) was added to a suspension of [{(η^6-biphenyl)$RuCl_2$}$_2$] (0.2 mmol, 0.130 g) in dry methanol (15 mL) and the reaction mixture was heated to reflux for 1 h at 85 °C. Then it was filtered, the resulting orange solution concentrated by rotary evaporation under reduced pressure to 1 mL, and a saturated solution of NH_4PF_6 in methanol (2–4 mL) was added. The yellow-ochre precipitate that formed immediately was collected by filtration, washed with water (1×2 mL) and diethyl ether (3×15 mL), and dried in vacuo. The ochre solid was redissolved in the minimum amount of methanol, and diethyl ether was added to precipitate 65 mg of the target complex as a yellow powder. The orange aqueous supernatant was left to stand at 0 °C for 8 h and orange microcrystals of the complex formed (15 mg, overall yield 43%). Crystals suitable for X-ray diffraction analysis (orange needles) were grown by slow diffusion of diethyl ether into a methanol solution.

Elemental analysis (%) calcd for $C_{12}H_{16}RuN_2PF_6Cl$ (469.76 g mol^{-1}): C 30.68, H 3.43, N 5.96; found: C 30.90, H 3.14, N 5.86%; MS (ESI+): *m/z* 308.0 [(η^6-biphenyl)$Ru(NH_3)Cl$]$^+$; found: 308.4; MS (ESI−): *m/z* 145.0 $[PF_6]^-$; found: 144.5; ^{1}H NMR (500.10 MHz; [D$_6$]DMSO): δ = 3.49 (s, 6H, NH_3), 5.82 (m, 3H, CH_{phen}), 6.11 (m, 2H, CH_{phen}), 7.51 (m, 3H, $RuCH_{phen}$), 7.80 ppm (m, 2H, $RuCH_{phen}$); ^{31}P NMR (202.44 MHz; [D$_6$]DMSO): δ = −144.24 ppm (sept, 1P, $^1J_{PF}$ = 711.7 Hz, PF_6).

*[(η^6-p-cymene)Ru^{II}(diethylenetriamine)]$Cl(PF_6)$ (**3a**)*: Diethylenetriamine (27 μL, 0.25 mmol) was added to a suspension of [{(η^6-*p*-cymene)$RuCl_2$}$_2$] (0.09 mmol, 0.056 g) in dry methanol (15 mL). The reaction mixture immediately turned into a light yellow solution, which was stirred for 1.5 h, filtered, and concentrated by rotary evaporation under reduced pressure to 1 mL, after which a saturated solution of NH_4PF_6 in methanol (2–4 mL) was added. The solution was filtered and diethyl ether (15 mL) added. The mixture was allowed to stand at 0 °C for 8 h, and the yellow precipitate was collected by filtration, washed with diethyl ether (3×15 mL), and dried in vacuo to yield 70 mg (75%) of the target complex. Crystals suitable for X-ray diffraction analysis were grown by slow diffusion of diethyl ether into a methanol solution.

Elemental analysis (%) calcd for $C_{14}H_{27}RuN_3PF_6Cl$ (518.87 g mol^{-1}): C 32.41, H 5.24, N 8.10; found: C 32.21, H 4.95, N 8.21%; MS (ESI+): *m/z* 338.1 [(η^6-*p*-cymene)Ru(diethylenetriamine)−H]$^+$; found: 337.9; MS

(ESI−): 145.0 $[PF_6]^-$; found: 144.8; ^{1}H NMR (500.10 MHz; [D$_6$]DMSO): δ = 1.21 (d, 6H, $^3J_{HH}$ = 6.9 Hz, CH(CH_3)$_2$), 2.25 (s, 3H, C$_6$H$_4$(CH_3)), 2.48–2.55 (m, 4H, C$_2$H$_4$), 2.61(m, 2H, C$_2$H$_4$), 2.76 (m, 2H, C$_2$H$_4$), 2.96 (sept, 1H, $^3J_{HH}$ = 6.9 Hz, C*H*Me$_2$), 5.14 (m, 2H, NH$_2$), 5.61 (d, 2H, $^3J_{HH}$ = 6.2 Hz, CH$_{cym}$), 5.73 (d, 2H, $^3J_{HH}$ = 6.2 Hz, CH$_{cym}$), 6.48 (m, 2H, NH$_2$), 7.92 ppm (m, 1H, NH); ^{31}P NMR (202.44 MHz; [D$_6$]DMSO): δ = −144.22 ppm (sept, 1P, $^1J_{PF}$ = 720.6 Hz, PF$_6$).

[(η^6-biphenyl)Ru^{II}(diethylenetriamine)](PF$_6$)$_2$ (***3b***): [{(η^6-biphenyl)-RuCl$_2$}$_2$] (0.14 mmol, 0.091 g) was heated to reflux in water/methanol (10:1) at 85 °C for 2 h and then cooled to 55 °C. Diethylenetriamine (38 μL, 0.35 mmol) was added to this suspension, which turned from red-brown to yellow-greenish. This was then slowly heated to reflux again for another 1.5 h and filtered while hot. The resulting yellow solution was then concentrated by rotary evaporation under reduced pressure to 1 mL, and a saturated solution of NH_4PF_6 in water (2–4 mL) was added. The flask was briefly shaken, and a light-yellow precipitate immediately formed. The mixture was allowed to stand at 0 °C for 8 h, the precipitate was collected by filtration, washed with water (2×2 mL) and diethyl ether (3×15 mL), and dried in vacuo to yield 98 mg (54 %) of the target complex.

Elemental analysis (%) calcd for $C_{16}H_{23}RuN_3P_2F_{12}$ (648.37 g mol^{-1}): C 29.64, H 3.58, N 6.48; found: C 29.54, H 3.20, N 6.25 %; MS (ESI+): *m/z* 358.1 [(η^6-biphenyl)Ru(diethylenetriamine)−H]$^+$; found: 357.9; MS (ESI−): 145.0 $[PF_6]^-$; found: 144.8; ^{1}H NMR (500.10 MHz; [D$_6$]DMSO): δ = 2.41 −2.60 (m, 4H, C$_2H_4$), 2.72 (m, 4H, C$_2H_4$), 4.31 (m, 2H, NH_2), 5.92 (t, 2H, $^3J_{HH}$ = 6.0 Hz, CH$_{phen}$), 6.04 (t, 1H, $^3J_{HH}$ = 5.7 Hz, CH$_{phen}$), 6.30 (d, 2H, $^3J_{HH}$ = 6.0 Hz, CH$_{phen}$), 5.92 (m, 2H, NH$_2$), 7.55 (m, 3H, RuCH$_{phen}$), 7.80 (m, 2H, RuCH$_{phen}$), 8.32 ppm (m, 1H, NH); ^{31}P NMR (202.44 MHz; [D$_6$]DMSO): δ = −144.19 ppm (sept, 1P, $^1J_{PF}$ = 711.3 Hz, PF$_6$).

[(η^6-biphenyl)Ru^{II}(ethylenediamine)(NH$_3$)](PF$_6$)$_2$ (***4b***): A solution of $AgPF_6$ (0.11 mmol, 0.028 g) in methanol (2 mL) was added to a solution of [(η^6-biphenyl)Ru(ethylenediamine)Cl]PF$_6$ (0.1 mmol, 0.050 g) in dry methanol (7 mL) and the mixture stirred for 2 h. A white precipitate of AgCl was quickly filtered off under aerobic conditions and the resulting solution was flushed with Ar. Ammonia gas was bubbled through the solution, which caused significant warming of the reaction mixture with no color change. After the clear solution had cooled the gas supply was stopped and the reaction mixture was stirred for 1 h. The yellow solution was filtered, concentrated to 1 mL by rotary evaporation under reduced pressure, and a saturated solution of NH_4PF_6 in water (2–4 mL) was added. A green-yellow precipitate formed immediately, which was collected by filtration, washed with water (2×2 mL) and diethyl ether (3×15 mL) and dried in vacuo to yield 21 mg (33 %) of the target complex. Crystals suitable for X-ray diffraction analysis were grown by slow diffusion of diethyl ether into a methanol solution.

Elemental analysis (%) calcd for $C_{14}H_{21}RuN_3P_2F_{12}$·0.5 CH_3OH (638.36 g mol^{-1}): C 27.28, H 3.63, N 6.58; found: C 27.59, H 3.89, N 6.59 %; MS (ESI+): *m/z* 315.0 [(η^6-biphenyl)Ru(diethylenediamine)−H]$^+$; found: 315.1; MS (ESI−): *m/z* 145.0 $[PF_6]^-$; found: 144.9; ^{1}H NMR (500.10 MHz; [D$_6$]DMSO): δ = 2.18 (m, 2H, CH$_2$), 2.34 (m, 2H, CH$_2$), 3.51 (s, 3H, NH$_3$), 4.30 (m, 2H, NH$_2$), 5.89 (t, 2H, $^3J_{HH}$ = 6.0 Hz CH$_{phen}$), 5.97 (t, 1H, $^3J_{HH}$ = 5.6 Hz, CH$_{phen}$), 6.23 (d, 2H, $^3J_{HH}$ = 6.1 Hz, CH$_{phen}$), 6.41 (m, 2H, NH_2), 7.57 (m, 3H, RuCH$_{phen}$), 7.76 ppm (m, 2H, RuCH$_{phen}$); ^{31}P NMR (202.44 MHz; [D$_6$]DMSO): δ = −143.18 ppm (sept, 1P, $^1J_{PF}$ = 720.5 Hz, PF$_6$).

*[(η^6-p-cymene)Ru^{II}(NH$_3$)Cl$_2$][(dmbaH)(PF$_6$)] (**5a**)*: The procedure of Betanzos-Lara et al.[17] was used after minor modification. In brief, *N,N*-dimethylbenzylamine (dmba, 0.098 mL, 0.65 mmol) and NH_4PF_6 (0.106 g, 0.65 mmol) were added to a suspension of [{(η^6-*p*-cymene)RuCl$_2$}$_2$] (0.32 g, 0.2 mmol) in dry methanol (15 mL) and the reaction mixture was stirred for 18 h at room temperature. Then it was filtered and the resulting orange solution evaporated to dryness. The oily residue was redissolved in the minimum amount of CH_2Cl_2 and diethyl ether (30 mL) added. The flask was briefly shaken, and a light yellow precipitate immediately formed. The mixture was allowed to stand at 0 °C for 8 h, and the precipitate was collected by filtration, washed with diethyl ether (3× 15 mL), and dried in vacuo to yield 155 mg (64 %) of the target complex.

Elemental analysis (%) calcd for $C_{19}H_{31}RuN_2Cl_2PF_6$ (604.40 g mol^{-1}): C 37.75, H 5.17, N 4.63; found: C 37.58, H 5.46, N 4.96 %; MS (ESI+): *m/z* 136.1 [dmba+H]$^+$, 289.0 {[(η^6-*p*-cymene)Ru(NH$_3$)Cl]$^+$+[(η^6-*p*-cymene)Ru(NH$_3$)Cl+H]$^+$}; found: 136.6, 289.3; MS (ESI−): *m/z* 145.0 $[PF_6]^-$; found: 144.5; ^{1}H NMR (500.10 MHz; CD_3NO_2): δ = 1.31 (d, 6H, $^3J_{HH}$ = 7.0 Hz, CH(CH_3)$_2$), 2.10 (s, 3H, C$_6$H$_4$(CH_3)), 2.90 (sept, 1H, $^3J_{HH}$ = 7.0 Hz, C*H*Me$_2$), 2.74 (s, 3H, NH$_3$), 2.94 (s, 6H, N(CH_3)$_2$) 4.38 (s, 2H, CH$_2$), 5.35 (d, 2H, $^3J_{HH}$ = 6.0 Hz, CH$_{cym}$), 5.56 (d, 2H, $^3J_{HH}$ = 6.0 Hz, CH$_{cym}$), 7.53 (m, 3H, CH$_{dmba}$), 7.58 ppm (m, 2H, CH$_{dmba}$); ^{31}P NMR (202.44 MHz; CD_3NO_2): δ = −146.53 ppm (sept, 1P, $^1J_{PF}$ = 734.1 Hz, PF$_6$).

*[(η^6-biphenyl)Ru^{II}(NH$_3$)Cl$_2$][(dmbaH)(PF$_6$)] (**5b**)*: [{(η^6-biphenyl)RuCl$_2$}$_2$] (0.3 mmol, 0.196 g) was heated to reflux in methanol (80 mL) at 85 °C for 2 h and then cooled to room temperature. *N,N*-Dimethylbenzylamine (0.09 mL, 0.6 mmol) and NH_4PF_6 (0.98 g, 0.6 mmol) were added to the brown solution and the reaction mixture was stirred for 18 h at ambient temperature while no color change occurred. The solution was filtered and the orange-brown filtrate was evaporated to dryness. The oily residue was redissolved in a minimum amount of CH_2Cl_2 and 30 mL of diethyl ether was added. The precipitate was collected by filtration, washed with diethyl ether (3×15 mL), and dried in vacuo to yield 123 mg (33 %) of the target complex.

Elemental analysis (%) calcd for $C_{21}H_{27}RuN_2Cl_2PF_6$ (624.39 g mol^{-1}): C 40.40, H 4.36, N 4.49; found: C 40.22, H 4.46, N 4.50 %; MS (ESI+): *m/z* 136.1 [dmba+H]$^+$, 308.0 [[(η^6-biphenyl)Ru(NH$_3$)Cl]$^+$; found: 136.3, 308.3; MS (ESI−): *m/z* 145.0 $[PF_6]^-$; found: 144.6; ^{1}H NMR (500.10 MHz; CD_3NO_2): δ = 2.18 (br, 3H, NH$_3$), 2.88 (s, 6H, N(CH$_3$)$_2$) 4.14 (s, 2H, CH$_2$), 5.97 (m, 2H, CH$_{phen}$), 5.76 (m, 2H, CH$_{phen}$), 7.51 (m, 3H, RuCH$_{phen}$), 7.58 (m, 5H, CH$_{dmba}$), 7.79 ppm (m, 2H, RuCH$_{phen}$); ^{31}P NMR (202.44 MHz; [D$_6$]DMSO): δ = −144.15 ppm (sept, 1P, $^1J_{PF}$ = 746.7 Hz, PF$_6$).

*[(η^6-p-cymene)Ru^{II}(NH$_3$)Cl$_2$][(Et$_3$NH)(PF$_6$)] (**6a**)*: Triethylamine (0.090 mL, 0.65 mmol) and NH_4PF_6 (0.106 g, 0.65 mmol) were added to a suspension of [{(η^6-*p*-cymene)RuCl$_2$}$_2$] (0.32 g, 0.2 mmol) in dry methanol (15 mL) and the reaction mixture was stirred for 18 h at room temperature. Then it was filtered and the resulting orange solution was concentrated to 2 mL, whereby it turned dark brown. The solution was filtered again and crystals suitable for X-ray diffraction analysis (long brown needles) were grown by slow diffusion of diethyl ether into a dichloromethane solution. The crystals were manually separated from the brown residue and washed with diethyl ether (5×15 mL) to give 80 mg (35 %) of the target product.

Elemental analysis (%) calcd for $C_{16}H_{33}RuN_2Cl_2PF_6$ (570.39 g mol^{-1}): C 33.69, H 5.83, N 4.91; found: C 33.40, H 6.20, N 4.86 %; MS (ESI+): *m/z* 102.2 [Et$_3$N+H]$^+$, 270.7 [(η^6-*p*-cymene)RuCl]$^+$, 289.0 {[(η^6-cymene)Ru(NH$_3$)Cl]$^+$+[(η^6-*p*-cymene)Ru(NH$_3$)Cl+H]$^+$}; found: 102.6, 271.1, 289.1; MS (ESI−): *m/z* 145.0 $[PF_6]^-$; found: 144.5; ^{1}H NMR (500.10 MHz; CD_3NO_2): δ = 1.30 (d, 6H, $^3J_{HH}$ = 7.0 Hz, CH(CH_3)$_2$), 1.37 (t, 9H, $^3J_{HH}$ = 7.3 Hz, CH_3), 2.19 (s, 3H, C$_6$H$_4$(CH_3)), 2.88 (sept, 1H, $^3J_{HH}$ = 6.9 Hz, C*H*Me$_2$), 2.71 (s, 3H, NH_3), 3.34 (m, 6H, CH$_2$), 5.31 (d, 2H, $^3J_{HH}$ = 5.9 Hz, CH$_{cym}$), 5.53 ppm (d, 2H, $^3J_{HH}$ = 5.9 Hz, CH$_{cym}$); ^{31}P NMR (202.44 MHz; CD_3NO_2): δ = −146.53 ppm (sept, 1P, $^1J_{PF}$ = 737.0 Hz, PF$_6$).

Results and Discussion

Synthesis of organoruthenium(II) am(m)ine complexes: Numerous studies on Ru^{II} η^6-arene complexes with different numbers of coordinated ammine ligands have been published[17,23] since the first report of the synthesis of [(η^6-benzene)Ru(NH$_3$)$_2$Cl](PF$_6$)$_3$·NH$_4$PF$_6$ in 1978[23b] until the most recent publications.[17,23g] Despite the variety of synthetic pathways, some of them are contradictory.[23a,c,d] We found that the type of products, that is, with two ammine ligands in [(η^6-arene)Ru(NH$_3$)$_2$Cl](PF$_6$) or three in [(η^6-arene)Ru(NH$_3$)$_3$](PF$_6$)$_2$, and their yields strictly depend on

the reaction conditions, such as temperature and reaction time, concentration of the reactants, and quality of the solvents.

All of the complexes were synthesized from the ruthenium precursors $[\{(\eta^6\text{-arene})RuCl_2\}_2]$ (**A**: arene = *p*-cymene; **B**: arene = biphenyl). Dimeric complex **B** has low solubility in most commonly used solvents. Therefore, in general, reactions involving the η^6-biphenyl fragment require longer reaction times and additional purification steps and resulted in lower yields in comparison to η^6-*p*-cymene complexes. The metal species formed during the reaction are highly reactive and can be stabilized by coordination of solvent molecules which are quickly substituted by nitrogen ligands with higher affinity to ruthenium. It was reported that solvents of medium polarity, such as methanol and nitromethane, yield the target complexes in higher yields,[17] a fact also observed in our studies. The generated compounds with labile chlorido ligands can be easily hydrolyzed, and therefore synthesis and isolation were performed in absolute solvents.

It was recently reported that the reaction of **A** and **B** with aqueous ammonia results in a mixture of products.[23g] However, by treating **A** and **B** with a large excess of 25% aqueous ammonia in refluxing methanol we obtained ruthenium complexes **1a** and **1b** with three ammonia ligands, which were unambiguously characterized by NMR spectroscopy and mass spectrometry. The reaction time does not affect the type of product, but the yield of the reaction. Indeed, a series of experiments was performed with refluxing or stirring the reagents for 1 or 24 h, and it was found that the maximum yield can be obtained after 1 h of reflux (64%) or 24 h of stirring (60%), while the yields after 1 h of stirring and 24 h of reflux were unsatisfactory (37 and 22%). Low or moderate yields of the reaction prompted the use of alternative sources of ammonia. Commercially available solutions of NH_3 in dioxane or ethanol were found to be inappropriate for preparing the desired compounds. However, reaction with ammonia gas bubbled through the reaction mixture yielded the target complexes in good yields (90 and 70% for **1a** and **1b**, respectively).

When ruthenium precursors **A** and **B** were heated to reflux with a slight excess of 25% aqueous ammonia for one hour, complexes with two ammonia and one chlorido ligand were formed in moderate yields (49 and 43% for **2a** and **2b**; Scheme 1). The optimal reaction time was found to be 1–3 h. However, the same reaction but with an equimolar amount of NH_3 did not lead to the target products **5a** and **5b** featuring one ammonia and two chlorido ligands. These complexes were successfully prepared by in situ generation of NH_3 from stoichiometric amounts of base (e.g, dimethylbenzylamine or triethylamine) and NH_4PF_6 and were always isolated as adducts of the complexes with the base.

Complexes **7a** and **7b** with bidentate ethylenediamine (en) ligand were synthesized according to a literature procedure.[19] Complex **4b** can be obtained in a single step from **7b** by removal of the chlorido ligand with silver salts and subsequent reaction with ammonia gas bubbled through the solution (yield: 33%). We also investigated the reactions of **A** and **B** with various tridentate ligands. Although osmium complexes with tridentate macrocycles such as 1,4,7-trimethyl-1,4,7-triazacyclononane and 1,4,7-triazacyclononane are known,[23f,24] similar reactions with the ruthenium precursors resulted in fast darkening of the solution and decomposition. However, we succeeded in the synthesis of ruthenium complexes with the tridentate ligand diethylenetriamine (dien), which readily forms a complex with dimer **A** on stirring for 1.5 h with an excess of the ligand (yield: 75%). The reaction of biphenyl precursor **B** under the same conditions resulted in the formation of **3b** in low yield. However, **3b** was obtained in 54% yield when **B** was heated to reflux for 2 h in water/methanol before an excess of dien was added, followed by stirring for 1.5 h at 55 °C.

All complexes were characterized by ^1H and ^{31}P NMR spectroscopy as well as ESI-MS and elemental analysis. The NH_3 protons of $[(\eta^6\text{-}p\text{-cymene})Ru(NH_3)_3](PF_6)_2$ (**1a**), $[(\eta^6\text{-biphenyl})Ru(NH_3)_3](PF_6)_2$ (**1b**), $[(\eta^6\text{-}p\text{-cymene})Ru(NH_3)_2Cl](PF_6)$ (**2a**), and $[(\eta^6\text{-biphenyl})Ru(NH_3)_2Cl](PF_6)$

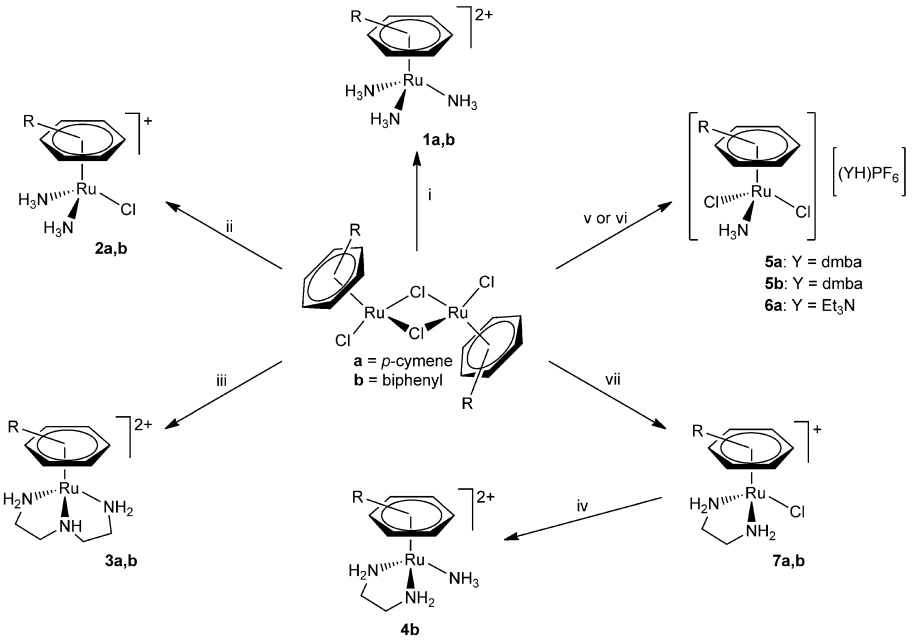

Scheme 1. Synthesis of Ru^{II} arene complexes with am(m)ine ligands. i) MeOH, $NH_{3,g}$, NH_4PF_6/MeOH or 25% NH_4OH excess, NH_4PF_6; ii) MeOH, 25% NH_4OH, NH_4PF_6; iii) MeOH, dien, NH_4PF_6; iv) MeOH, en, $NH_{3,g}$, $AgPF_6$, NH_4PF_6; v) MeOH, dmba, NH_4PF_6; vi) MeOH, Et_3N, NH_4PF_6; vii) MeOH, en, NH_4PF_6.[19]

(**2b**) appear as a broad singlet. The NH_3 proton resonances of cymene complexes are detected at a higher field (3.36 ppm) than those of biphenyl derivatives (3.49 ppm) because of the higher electron density at the Ru^{II} centers caused by the weaker π-accepting and stronger π-donating capability of *p*-cymene. The NH_3 signal has approximately the same chemical shift in [(η⁶-biphenyl)$Ru(NH_3)_3$]$(PF_6)_2$ (**1b**), [(η⁶-biphenyl)$Ru(NH_3)_2Cl$](PF_6) (**2b**), and [(η⁶-biphenyl)Ru(ethylenediamine)(NH_3)]$(PF_6)_2$ (**4b**).

The ^1H NMR spectrum of the free dien ligand was recorded in a variety of solvents (see Table S3 in the Supporting Information). The methylene protons gave rise to two sharp multiplets in all solvents, whereas NH and NH_2 protons appeared as sharp singlets at $\delta = 1.06$ and 4.83 ppm in $CDCl_3$ and CD_3OD, and as a broad singlet at $\delta = 1.44$ ppm in $[D_6]$DMSO. In D_2O, NH/NH_2 signals were not observed due to H/D exchange. On coordination to the metal center, the proton spectra undergo drastic changes, and the NH_2/NH protons are detected as three significantly downshifted signals (see Table S2 in the Supporting Information), indicating electron donation by the diethylenetriamine ligand to the Ru^{II} center. The NMR spectra of [(η⁶-*p*-cymene)Ru(dien)]$(PF_6)_2$ (**3a**) and [(η⁶-biphenyl)Ru(dien)]$(PF_6)_2$ (**3b**) were also recorded in various solvents, but no significant differences were found for the resonances of the arene rings. Methyl and methylene proton resonances were also insensitive to the nature of the solvent, unlike those of the amino groups. In both complexes, the NH/NH_2 proton resonances of coordinated diethylenetriamine recorded in $[D_6]$DMSO lie downfield ($\Delta\delta = 1.06$ and 0.57 ppm for **3a** and **3b**, respectively) with respect to those recorded in CD_3OD and D_2O. The NH/NH_2 protons of the diethylenetriamine ligand in **3a** and **3b** undergo slow H/D exchange in protic solvents (>48 h), but it can be accelerated by addition of NaOD to be complete within several minutes. The protons of the ammine ligands in **1a**, **1b**, **2a**, **2b**, and **4b** undergo fast H/D exchange (see Figure S1 in the Supporting Information), which results in the disappearance of the corresponding signals in the ^1H NMR spectra within several hours. Therefore, coordination of chelating triethylenetriamine results in a more pronounced reduction of the rate of H/D exchange in protic solvent compared to monodentate ammine ligands.

X-ray structure determination: The molecular structures of [(η⁶-biphenyl)$Ru^{II}(NH_3)_2Cl$](PF_6) (**2b**), [(η⁶-*p*-cymene)Ru^{II}(dien)]$(PF_6)(Cl)$ (**3a**), [(η⁶-biphenyl)Ru^{II}(en)(NH_3)]$(PF_6)_2$ (**4b**), and [(η⁶-*p*-cymene)$Ru^{II}(NH_3)Cl_2$][$(Et_3NH)(PF_6)$] (**6a**) were determined by X-ray diffraction analysis (Figures 1 and 2, see Tables S1 and S2 in the Supporting Information for crystallographic data, bond lengths, and bond angles). Single crystals of the complexes were grown by slow diffusion of diethyl ether into saturated methanol solutions at 277 K.

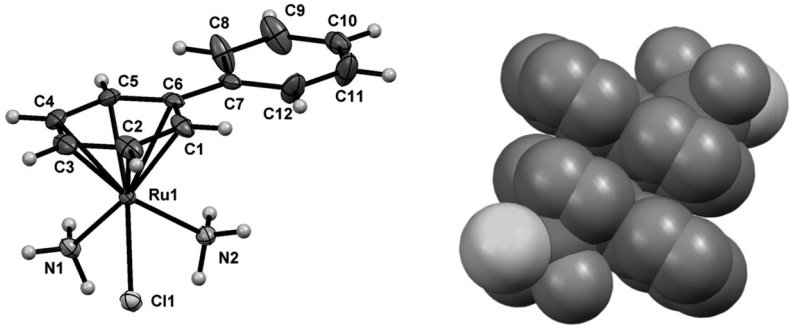

Figure 1. Molecular structure of [(η⁶-biphenyl)$Ru^{II}(NH_3)_2Cl$](PF_6) (**2b**, left) and space-filling model (right) showing π–π stacking interactions between the phenyl rings of two molecules. The PF_6^- anion has been omitted for clarity. Selected bond lengths [Å] and angles [°]: Ru1−C(1–6)$_{av}$ 2.1826(35), Ru1−Cl1 2.4125(4), Ru1−N1 2.1417(14), Ru1−N2 2.1324(14); N1-Ru1-Cl1 83.53(4), N2-Ru-Cl1 83.36(4), N1-Ru-N2 82.88(6).

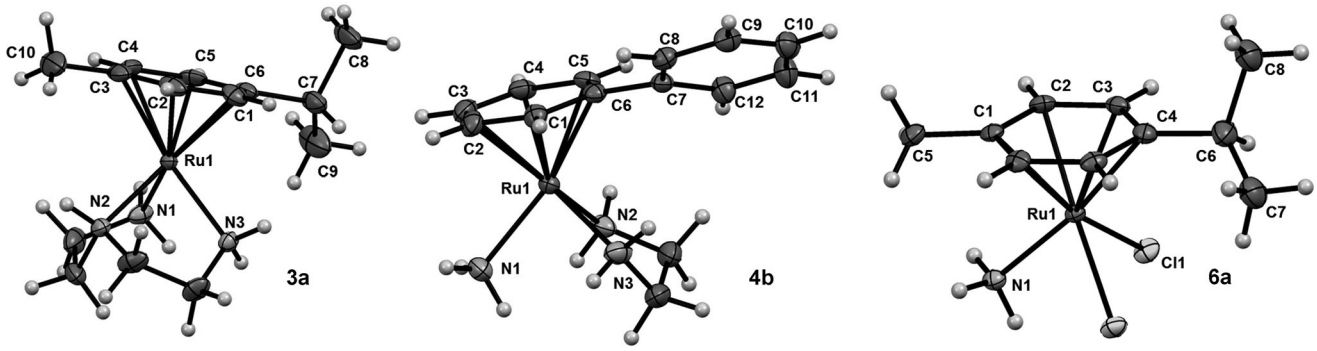

Figure 2. Molecular structures of dicationic [(η⁶-*p*-cymene)Ru^{II}(dien)]$(PF_6)_2$ (**3a**, left) and [(η⁶-biphenyl)Ru^{II}(en)(NH_3)]$(PF_6)_2$ (**4b**, center) and neutral [(η⁶-*p*-cymene)$Ru^{II}(NH_3)Cl_2$][$(Et_3NH)(PF_6)$] (**6a**, right). The PF_6^- anions and Et_3NH^+ were omitted for clarity. Selected bond lengths [Å] and angles [°] for **3a**: Ru1−C(1–6)$_{av}$ 2.190(1), Ru1−N1 2.120(5), Ru1−N2 2.127(5), Ru1−N3 2.130(5); N1-Ru1-N2 79.4(2), N3-Ru-N1 88.39(19), N2-Ru-N3 77.61(19). For **4b**: Ru1−C(1–6)$_{av}$ 2.1937(52), Ru1−N1 2.1515(17), Ru1−N2 2.1324(17), Ru1−N3 2.1388(17), N1-Ru1-N2 84.79(7), N3-Ru-N1 88.35(7), N2-Ru-N3 79.39(7). For **6a**: The complex cation contains a reflection plane passing through Ru1, N1, C1, C4, C5, and C6; Ru1−C(1–6)$_{av}$ 2.170(8), Ru1−Cl1 2.4157(6), Ru1−Cl2 2.4157(6), Ru1−N1 2.130(3); N1-Ru1-Cl1 83.26(6), N1-Ru1-Cl2 83.26(6), Cl1-Ru1-Cl2 85.10.

The pseudo-octahedral coordination environment of the Ru^{II} center consists of Cl^- (**2b**, **6a**), and NH_3 (**2b**, **4b**, **6a**) or chelating ligands (**3a**, **4b**) and the η^6-arene ring. The unit cell of **6a** also contains a triethylammonium hexafluorophosphate ion pair.

In general, the geometrical parameters of all complexes are very similar. The Ru–Cl bond length does not vary significantly with the coordinated arene [2.4125(4) Å for [(η^6-biphenyl)$Ru^{II}(NH_3)_2Cl](PF_6)$ (**2b**) and 2.4146(4) Å for [(η^6-cymene)$Ru^{II}(NH_3)_2Cl](PF_6)$ (**2a**)],[23g] which is in accordance with observations for the mono-ammine complexes [(η^6-arene)$Ru^{II}(NH_3)Cl_2$] (**5a**,**b**) (2.421(2), 2.427(2) and 2.4246(9), 2.4284(8) for cymene/biphenyl respectively).[17] In contrast, the Ru–Cl bond in the ethylenediamine complexes [(η^6-arene)Ru^{II}(en)Cl]PF_6 (**7a**,**b**) is remarkably longer in the cymene complex [2.4418(8) Å (**7a**) vs. 2.4080(15) Å (**7b**)].[19] The Ru–N bond lengths in **2b, 3a**, **4b**, and **6a** are in the range 2.120–2.152 Å, and N-Ru-N angles vary between 79 and 88°. These values are similar to those reported previously for related Ru^{II}(arene) complexes.[19,23g] The Ru–$Ph_{centroid}$ distance in **2b** (1.662 Å) is slightly longer than that of its cymene analogue **2a** (1.659 Å), which is again in accordance with mono-ammine complexes, although less pronounced (1.670 Å for **5b** vs. 1.657 Å for **5a**).[17] Furthermore, the slightly longer bond lengths for Ru–biphenyl correlate with the higher π acidity compared to *p*-cymene, which leads to a partial filling of the antibonding orbitals of the Ru–arene bonds. All structures feature longer Ru–$C_{substituted}$ than Ru–CH bonds. In the X-ray structure of **2b**, but not of **4b**, intermolecular π stacking was observed in a parallel offset fashion (Figure 1) with a shortest interatomic distance of 3.347 Å and a $Ph_{centroid}$···$Ph_{centroid}$ distance of 3.823 Å. In contrast to structurally related ruthenium(II) half-sandwich complexes bearing biphenyl moieties, in which one phenyl ring is twisted out of the plane by around 23.3(9)° (**7b**)[19] or 39.5(5)° (**5b**),[17] the biphenyl ligand in **2b** is surprisingly almost planar (0.3(3)°). In **4b**, the phenyl rings of the biphenyl ligand are tilted from coplanarity by 28.6(3)°.

Hydrolysis and stability studies: Hydrolysis and stability tests were carried out for the complexes prior to investigation of their reactivity toward biomolecules. The stability of the complexes was investigated in water and in 0.1 M (simulating blood plasma conditions) and 1 M aqueous NaCl solutions by means of ^{1}H NMR spectroscopy. It is known that **2a**,**b**,[23g] **5a**,**b**[19] and **7a**,**b**[17] form mono- and diaqua complexes in water through substitution of chlorido ligands with water molecules. While aquation of the ammine complexes **2a**,**b**, **5a**,**b** and **6a** was not suppressed even in 1 M NaCl solution, the ethylenediamine species **7a**,**b** remained intact for 24 h in 0.1 M NaCl. The complexes without labile chlorido ligands (i.e., **1a**,**b**, **3a**,**b** and **4b**) are inert toward hydrolysis in aqueous solution. In long-term stability studies (up to 90 d), a second set of peaks was observed in the NMR spectra after about 10 d (shifted upfield by ca. 0.3 ppm and at 6% relative intensity, see Figure S1 in the Supporting Information). The intensity of this set of peaks remained constant over the following 80 d, which is indicative of the establishment of an equilibrium. Off-line electrospray ionization mass spectrometry (ESI-MS) measurements of the NMR samples containing **1b** and **3b** showed identical species as observed after 24 h (see below). However, additional hydroxido- and methoxido-bridged dimers were detected in the mass spectrum of **1b**. This suggests that the above-mentioned hydrolysis products may be formed after ammine ligand cleavage.

Furthermore, the stability of the biphenyl compounds in aqueous solution was assayed by ESI-MS, which largely confirmed the observations made by NMR spectroscopy. However, labile monodentate ligands, such as ammine or chlorido, attached to a ruthenium center may be cleaved to a considerable extent even during the soft electrospray process. Such cleavage is observed at a dry gas temperature as low as 80 °C and leads to the formation of dinuclear hydrolysis products with bridging solvent molecules, which are usually regarded as an inactive form of Ru^{II} arene anticancer agents.[25] Accordingly, the most abundant signal in the mass spectrum of **2b** was assigned to a dinuclear hydrolysis product after cleavage of the monodentate ligands, namely, $[(bip)_2Ru_2(\mu\text{-}OCH_3)_3]^+$ (m/z 604.87 ± 0.1, m_{ex} = 605.02; bip = η^6-biphenyl), observed throughout the entire incubation period. Similar dinuclear methoxido-containing hydrolysis products were also observed in the mass spectra of **5b**. The methoxide ligands probably stem from the dilution process with water:methanol (1:1) prior to ESI-MS measurements. In case of **1b**, the most abundant signal was found at m/z 288.92 ± 0.01, corresponding to a $[(bip)Ru(NH_3)(NH_2)]^+$ fragment (m_{ex} = 289.03). The isotope pattern suggests an Ru^I/Ru^{II} redox couple in form of $[(bip)Ru(NH_3)_2]^+$ and $[(bip)Ru(NH_3)-H]^+$ and a ratio of 1:0.75, while dimeric hydrolysis products were not observed. Due to the lability of the investigated monodentate ligands under the conditions applied in the MS experiments, unequivocal conclusions could not be drawn on the stability of the complexes in aqueous solution. In contrast, complexes containing chelating di- or triamines (e.g., **3b**, **4b**, and **7b**) exhibited higher stability during the spraying process. Their mass spectra remained constant over the entire incubation period, and therefore these compounds are believed to be stable for at least 48 h in aqueous solution. The most abundant signals in the mass spectra of **7b** were assigned to $[(bip)Ru(en)Cl]^+$ (m/z 350.91 ± 0.01, m_{ex} = 351.02) and $[(bip)Ru(en)-H]^+$ (m/z 314.93 ± 0.01, m_{ex} = 315.04); the latter was also observed in the spectra of **4b**. This provides further proof of the lability of monodentate ammine ligands during the electrospray process, since no further assignable signals were detected for **4b**. The mass spectrum recorded for dicationic **3b** showed solely the doubly charged $[M]^{2+}$ ion (m/z 179.44 ± 0.01, m_{ex} = 179.55).

Reactivity toward proteins: Understanding the interaction of novel metallodrugs with proteins is of particular interest, since anticancer drugs are mostly administered intravenously into the blood stream, where they are exposed to plasma

proteins. Electrospray ionization mass spectrometry (ESI-MS) has proven to be a very suitable tool for the investigation and monitoring of such interactions. In this study, incubations were carried out at 2:1 compound-to-protein molar ratio in aqueous solution. The reactivity of **2b**, **3b**, and **7b** was investigated toward ubiquitin (ub), cytochrome c (cyt), and a mixture containing equimolar amounts of ub and cyt. The MS studies were carried out in high-resolution time-of-flight (ToF) mode. Mass spectra of the incubation mixtures were recorded under denaturing conditions by adding 50% methanol and 0.2% formic acid prior to injection to ensure proper unfolding and protonation of the protein. Because of the absence of labile ligands, **3b** was used as a negative control, and accordingly no protein adducts were observed when it was incubated with ub, cyt, or the ub–cyt mixture for 48 h.

Compound **2b** reacted readily with ub, and after 48 h extensive depletion of free ub (3%) in favor of mono- (45%) and bis-adducts (52%) was observed (Figure 3). The detected masses correspond to a mono-adduct of the type

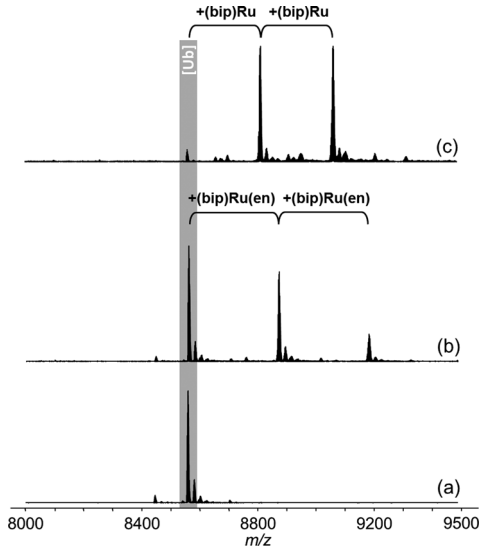

Figure 3. Deconvoluted mass spectra recorded for the incubation mixtures containing ub and **3b** (a), **7b** (b), or **2b** (c) after 48 h. The reaction mixtures were incubated at a compound-to-protein ratio of 2:1 at 37°C in the dark.

$[ub+(bip)Ru]^+$ (8818.6031 Da, m_{ex} = 8818.6051 Da, 0.2 ppm), while free ub was found at 8564.6299 Da (m_{ex} = 8564.6304 Da, 0.1 ppm) in the deconvoluted mass spectrum (Figure S2 of the Supporting Information), and a bis-adduct with two (bip)Ru moieties was detected at 9071.5659 Da (m_{ex} = 9071.5800 Da, 1.6 ppm). In case of **2b** the interaction with proteins is accompanied by cleavage of the ammine ligands, as observed previously with pyridonato complexes,[18d] although in-source ligand cleavage cannot be completely excluded (see above). The interaction between **2b** and cyt resulted in extensive metallation of the protein including higher order adducts at low abundance relative to cyt (12358.4023 Da, m_{ex} = 12358.3405 Da, 5 ppm). In particular, adducts corresponding to $[cyt+Ru(HCOO)]^+$ (12504.3070 Da, m_{ex} = 12504.2310 Da, 6 ppm, 15%), $[cyt+(bip)Ru]^+$ (12613.3526 Da, m_{ex} = 12613.3244 Da, 2 ppm, 26%), and $[cyt+(bip)Ru+Ru(HCOO)]^+$ (12757.2472 Da, m_{ex} = 12757.1985 Da, 4 ppm, 18%) were detected after 48 h. Similar to the stability studies, no adducts bearing monodentate ammine ligands were observed. Of interest is the observation of the signal at 12504.33 Da. A previous study attributed this signal to $[cyt+PF_6^-]$ (12505 Da).[23f] However, in the present case, the high-resolution mass spectrometric data and isotopic distribution suggest that it rather corresponds to a $[cyt+Ru(HCOO)]^+$ adduct (12504.23 Da), in which all of the ligands including the arene were cleaved (see Figure S2 in the Supporting Information). This may be related to oxidation of ruthenium to an Ru^{III} species. This difference in adduct formation between the two data sets may be attributed to differences in experimental conditions. Low metal (and therefore PF_6^-) concentrations and small metal-to-protein molar ratios thereby seem to favor formation of the $[cyt+Ru(HCOO)]^+$ adduct. Additionally, no comparable adduct was observed in the reaction with ub. The reaction of **2b** with a 1:1 ub:cyt mixture yielded similar results to the single-protein incubations. Complex **2b** seems to bind preferentially to ub forming mainly $[ub+(bip)Ru]^+$ mono-adducts, whereas mono-adduct formation with cyt was only observed at low relative abundance (Table 1).

Compound **7b** formed monofunctional adducts with ub of the type $[ub+(bip)Ru(en)]^+$ (8878.6821 Da, m_{ex} = 8878.6676 Da, 2 ppm, 42%), as reported for the undecapeptide substance P.[26] Retention of the ethylenediamine ligand is related to the stability of the coordinative bond between the *N*,*N*-bidentate ligand and the Ru center. In addition, the bis-adduct $[ub+2(bip)Ru(en)]^+$ (9191.7175 Da, m_{ex} = 9191.7038 Da, 2 ppm, 15%) was detected after 48 h. Incubation of **7b** with cyt yielded several metal–protein adducts within 48 h, and both mono- and bis-adducts were observed in considerable quantities. Similar to ub, these adducts corresponded to the $[(bip)Ru(en)]^+$ moiety attached to the pro-

Table 1. List of the detected metallodrug–protein adducts and their associated relative intensities during 2:1 incubation of **2b**, **3b**, or **7b** with ubiquitin (ub), cytochrome c (cyt), or an ub–cyt mixture after 48 h.

Compound	ub		cyt		ub–cyt mixture	
	adduct type	*I* [%]	adduct type	*I* [%]	adduct type	*I* [%]
2b	+(bip)Ru	45	+(bip)Ru	26	ub+(bip)Ru	84
	+2(bip)Ru	52	+Ru(HCOO)	15	ub+2(bip)Ru	5
			+(bip)Ru+Ru(HCOO)	18	cyt+(bip)Ru	9
3b	–		–		–	
7b	+(bip)Ru(en)	42	+(bip)Ru(en)	30	ub+(bip)Ru(en)	22
	+2(bip)Ru(en)	15	+2(bip)Ru(en)	6	cyt+(bip)Ru(en)	13
			+Ru(HCOO)	8		

tein, that is, $[cyt+(bip)Ru(en)]^+$ (12672.4068 Da, m_{ex} = 12672.3790 Da, 2 ppm, 30%) and $[cyt+2(bip)Ru(en)]^+$ (12986.4451 Da, m_{ex} = 12986.4169 Da, 2 ppm, 8%). Like for **2b**, the $[cyt+Ru(HCOO)]^+$ adduct was observed, albeit at low abundance (Table 1). When **7b** was incubated with the ub–cyt mixture, it reacted primarily with ub to form $[ub+(bip)Ru(en)]^+$, similarly to **2b**, whereas the analogous cyt adducts are much less pronounced.

In analogy to the proposed inverse correlation between extent of protein binding of a metallodrug and cytotoxic activity,[18g] **2b** is expected to be only active to a limited extent in in vitro assays due to pronounced binding to proteins and ligand cleavage. In contrast, **7b** displays a reduced rate of binding to proteins and also retains the ligand, which is anticipated to result in elevated anticancer activity. Compound **3b** does not react at all with proteins and would in principle be expected to show increased cytotoxicity. However, the absence of a leaving group does not allow conclusions on antitumor properties to be made in this case.

Interaction with 9-ethylguanine as a model for DNA binding: DNA binding is responsible for the antitumor activity of platinum anticancer agents.[14b] To evaluate the binding capability of representative complexes to DNA, **2b**, **5b**, and **7b** were treated with the DNA model 9-ethylguanine (EtG) and the reaction mixtures were analyzed by ESI-MS. In contrast to **5b** and **2b**, for which no interaction with EtG was observable, **7b** interacts specifically with the model purine. Mono-adducts are believed to form through hydrolysis of the chlorido leaving group and subsequent coordination of EtG to the Ru^{II} center. ESI-IT mass spectra featured peaks assignable to $[(bip)Ru(en)(EtG)PF_6]^+$ (m/z 639.93 ± 0.01, m_{ex} = 640.10), $[(bip)Ru(en)(EtG)]^+$ (m/z 493.97 ± 0.01, m_{ex} = 494.12), and $[(bip)Ru(en)(EtG)]^{2+}$ (m/z 247.45 ± 0.01, m_{ex} = 247.57), as well as free EtG (m/z 180.01 ± 0.01). CID tandem mass spectrometric experiments on the parent signal at m/z 494 gave peaks at m/z 180.01 and 314.93 for EtG and $[(bip)Ru(en)]^+$, respectively, confirming adduct formation of **7b** with EtG. The total percentage of signals attributable to **7b**–EtG adducts increased from 12% after 3 h to 78% after 48 h compared to all signals assigned to free **7b** (Table S4 in the Supporting Information). The stability of the **7b**–DNA adducts may be related to additional C6=O···HN hydrogen-bond formation between guanine and the ethylenediamine ligand.[27]

Inhibition of cancer cell growth: The in vitro anticancer activity of the Ru complexes was determined in ovarian (CH1), colon (SW480), and non-small cell lung carcinoma (A549) cells by means of the colorimetric MTT assay with an exposure time of 96 h (see Table 2 for IC_{50} values; concentration–effect curves are shown in Figure S3 in the Supporting Information). CH1 cells are significantly more chemosensitive to the complexes under investigation than SW480 and A549 cells. In general, the biphenyl complexes are more cytotoxic than their *p*-cymene counterparts,[16b] and only in case of **7a** and **7b** were both compounds approximately equally potent in all cell lines, with IC_{50} values mostly lower than 10 μM. This might be related to improved accumulation of more lipophilic complexes in cells, facilitated by diffusion of such compounds across membrane barriers. Furthermore, the arene ligand influences the reaction with biological targets. Biphenyl complexes may undergo π–π stacking interactions with nucleobases, leading to intercalation into DNA. However, it seems that the cytotoxicity of the compounds is strongly related to their ability to form covalent bonds, and indeed complexes with labile chlorido ligands were found to undergo quick aquation and yield the lowest IC_{50} values in the in vitro assays (**2b**, **7a**, **7b**), whereas **1a**, **1b**, **3a**, **3b**, and **4b** with three monodentate ammine or a tridentate amine ligand are virtually noncytotoxic, which may be attributed to the absence of a leaving group. Interestingly, **4b** shows medium in vitro activity, but seems drastically more active in CH1 and SW480 cell lines than **1a**,**b** and **3a**,**b**. This may be due to the monodentate ammine ligand, which under cellular conditions may nonetheless be cleaved. The resulting complex is then identical to hydrolyzed **7b**. However, the doubly charged complexes are expected to show less efficient cellular uptake compared to **2b** and **7a**,**b** and therefore reduced cytotoxicity. These results also confirmed the predictions from protein binding assays. On the contrary, the low activity of **2a**, **5a**, **5b**, and **6a** may be attributed to their instability in organic and especially in aqueous media, in which hydrolysis is not suppressible even by addition of 1 M NaCl, and side reactions may occur already in the cell culture medium prior to contact with the cells. This may also explain why the presence of two labile chlorido ligands (**5a**, **5b**, and **6a**) does not seem to be more advantageous than the presence of only one (**2a**, **2b**) despite the charge of the latter complexes, although the presence of two labile ligands is one of the prerequisites for the strong cytotoxicity of cisplatin (Table 2). Remarkably, neutral ruthenium complexes **5a** and **6a**, which contain noncova-

Table 2. Cytotoxicity of ruthenium complexes **1**–**7** and cisplatin given as 50% inhibitory concentrations (IC_{50}) in CH1 (ovarian carcinoma), A549 (non-small cell lung cancer), and SW480 (colon carcinoma) cells, determined by means of the MTT assay. Values are means plus/minus standard deviations obtained from at least three independent experiments with exposure times of 96 h.

Compound	IC_{50} [μM]		
	CH1	SW480	A549
1a	404 ± 29	474 ± 9	550 ± 16
1b	91 ± 17	272 ± 20	494 ± 54
2a	400 ± 20	586 ± 15	> 640
2b	3.3 ± 0.3	16 ± 2	68 ± 11
3a	> 640	> 640	> 640
3b	54 ± 5	204 ± 16	376 ± 20
4b	30 ± 3	78 ± 8	258 ± 12
5a	258 ± 21	360 ± 26	> 640
5b	85 ± 13	298 ± 21	566 ± 8
6a	343 ± 50	454 ± 19	580 ± 8
7a	7.3 ± 0.1	5.9 ± 0.7	8.8 ± 0.4
7b	6.2 ± 0.5	12 ± 2	9.2 ± 1.9
cisplatin[28]	0.14 ± 0.03	3.3 ± 0.4	1.3 ± 0.4

lently bound base–HPF_6 ion pairs, show a difference in cytotoxicity, which may depend on the base strength, whereby the former is slightly more active.

Conclusion

Ruthenium arene complexes of the bidentate ligand ethylenediamine are potent anticancer agents and have the potential to overcome resistance of tumors to cisplatin. In a systematic study by varying the am(m)ine and arene ligands of Ru half-sandwich compounds, several important parameters for structure–activity relationships could be derived when evaluating the in vitro anticancer activity of the compounds in human tumor cell lines (CH1, A549, and SW480). The cytotoxicity of the complexes strongly depends on the denticity of the ligand, and IC_{50} values varying by several orders of magnitude were observed. The activity of the complexes appears to be related to their aqueous stability. It is known that classic metal-based drugs serve as prodrugs and are activated by aquation to undergo interactions with biomolecules and exert antiproliferative activity. Inside the cell, activation can be achieved by slow hydrolysis of anionic ligands such as chloride in environments of low chloride concentration, while outside the cell the higher chloride ion concentration shifts the equilibrium to the chlorido complex, preventing formation of the active species. Compounds which are quickly hydrolyzed in aqueous (NaCl-containing) solution were found to be inactive in the anticancer assays, as were compounds which are too reactive towards proteins. These properties are of relevance to incubation with tumor cells in cell culture medium. These observations are in line with previous reports on organoruthenium complexes with three monodentate ligands such as acetonitrile or isonicotinamide,[19] and also with some more weakly bonding bidentate ligands.[18a,c,g] Furthermore, compounds lacking leaving groups were less active due to their too high stability. Overall, these facts indicate the necessity of covalent bond formation of the anticancer agent with the intracellular target for exerting anticancer activity.

Acknowledgements

This work was supported by the Platform Austria for Chemical Biology of the Genome Research Program Austria (GEN-AU, BMWF-70.081/0018-II/1a/2008), COST D39, and CM0902. We gratefully acknowledge Prof. Vladimir Arion for the refinement of X-ray diffraction data and Prof. Markus Galanski for recording the 2D NMR spectra.

[1] B. Rosenberg, L. VanCamp, J. E. Trosko, V. H. Mansour, *Nature* **1969**, *222*, 385–386.
[2] a) P. Koepf-Maier, *Eur. J. Clin. Pharmacol.* **1994**, *47*, 1–16; b) F. Caruso, M. Rossi, *Met. Ions Biol. Syst.* **2004**, *42*, 353–384.
[3] a) M. J. Clarke, *Coord. Chem. Rev.* **2003**, *236*, 209–233; b) Y. K. Yan, M. Melchart, A. Habtemariam, P. J. Sadler, *Chem. Commun.* **2005**, 4764–4776; c) I. Kostova, *Recent Pat. Anti-Cancer Drug Discovery* **2006**, *1*, 1–22; d) I. Bratsos, A. Bergamo, G. Sava, T. Gianferrara, E. Zangrando, E. Alessio, *J. Inorg. Biochem.* **2008**, *102*, 606–617.
[4] a) J. M. Rademaker-Lakhai, D. Van Den Bongard, D. Pluim, J. H. Beijnen, J. H. M. Schellens, *Clin. Cancer Res.* **2004**, *10*, 3717–3727; b) C. G. Hartinger, M. A. Jakupec, S. Zorbas-Seifried, M. Groessl, A. Egger, W. Berger, H. Zorbas, P. J. Dyson, B. K. Keppler, *Chem. Biodiversity* **2008**, *5*, 2140–2155; c) D. Thompson, G. J. Weiss, S. F. Jones, H. A. Burris, K. Ramanathan, J. R. Infante, J. C. Bendell, A. Ogden, D. D. von Hoff, at *ASCO Annual Meeting* **2012**, Abstract 3033.
[5] a) M. J. Clarke, S. Bitler, D. Rennert, M. Buchbinder, A. D. Kelman, *J. Inorg. Biochem.* **1980**, *12*, 79–87; b) P. Schluga, C. G. Hartinger, A. Egger, E. Reisner, M. Galanski, M. A. Jakupec, B. K. Keppler, *Dalton Trans.* **2006**, 1796–1802.
[6] M. A. A. F. d. C. T. Carrondo, W. P. Griffith, J. P. Hall, A. C. Skapski, *Biochim. Biophys. Acta Gen. Subj.* **1980**, *627*, 332–334.
[7] a) W. L. Ying, J. Emerson, M. J. Clarke, D. R. Sanadi, *Biochemistry* **1991**, *30*, 4949–4952; b) C. Zazueta, G. Zafra, G. Vera, C. Sanchez, E. Chavez, *J. Bioenerg. Biomembr.* **1998**, *30*, 489–498; c) C. Zazueta, M. E. Sosa-Torres, F. Correa, A. Garza-Ortiz, *J. Bioenerg. Biomembr.* **1999**, *31*, 551–557.
[8] C. M. Bastos, K. A. Gordon, T. D. Ocain, *Bioorg. Med. Chem. Lett.* **1998**, *8*, 147–150.
[9] D. Frasca, J. Ciampa, J. Emerson, R. S. Umans, M. J. Clarke, *Met.-Based Drugs* **1996**, *3*, 197–209.
[10] F. Bottomley, *Can. J. Chem.* **1977**, *55*, 2788–2791.
[11] a) K. A. Marx, R. Kruger, M. J. Clarke, *Mol. Cell. Biochem.* **1989**, *86*, 155–162; b) K. A. Marx, C. Seery, P. Malloy, *Mol. Cell. Biochem.* **1989**, *90*, 37–45.
[12] a) M. J. Clarke, *ACS Symp. Ser.* **1980**, *140*, 157–180; b) M. J. Clarke, F. Zhu, D. R. Frasca, *Chem. Rev.* **1999**, *99*, 2511–2533.
[13] a) J. E. Earley, P. M. Smith, T. Fealey, J. V. Silverton, *Inorg. Chem.* **1971**, *10*, 1943–1947; b) P. Nagababu, J. N. L. Latha, S. Satyanarayana, *Chem. Biodiversity* **2006**, *3*, 1219–1229; c) S. P. Mulcahy, K. Gruendler, C. Frias, L. Wagner, A. Prokop, E. Meggers, *Dalton Trans.* **2010**, *39*, 8177–8182; d) M. Shilpa, P. Nagababu, Y. P. Kumar, J. N. L. Latha, M. R. Reddy, K. S. Karthikeyan, N. Gabra, S. Satyanarayana, *J. Fluoresc.* **2011**, *21*, 1155–1164.
[14] a) S. van Zutphen, J. Reedijk, *Coord. Chem. Rev.* **2005**, *249*, 2845–2853; b) Y. Jung, S. J. Lippard, *Chem. Rev.* **2007**, *107*, 1387–1407.
[15] a) I. Bratsos, S. Jedner, T. Gianferrara, E. Alessio, *Chimia* **2007**, *61*, 692–697; b) C. G. Hartinger, P. J. Dyson, *Chem. Soc. Rev.* **2009**, *38*, 391–401; c) G. Sava, A. Bergamo, P. J. Dyson, *Dalton Trans.* **2011**, *40*, 9069–9075.
[16] a) R. E. Morris, P. J. Sadler, H. Chen, D. Jodrell, Half-sandwich ruthenium(II) compounds comprising nitrogen containing ligands for treatment of cancer, **2001**, WO2001030790 A1; b) A. Habtemariam, M. Melchart, R. Fernandez, S. Parsons, I. D. H. Oswald, A. Parkin, F. P. A. Fabbiani, J. E. Davidson, A. Dawson, R. E. Aird, D. I. Jodrell, P. J. Sadler, *J. Med. Chem.* **2006**, *49*, 6858–6868.
[17] S. Betanzos-Lara, A. Habtemariam, G. J. Clarkson, P. J. Sadler, *Eur. J. Inorg. Chem.* **2011**, 3257–3264.
[18] a) W. Kandioller, C. G. Hartinger, A. A. Nazarov, C. Bartel, M. Skocic, M. A. Jakupec, V. B. Arion, B. K. Keppler, *Chem. Eur. J.* **2009**, *15*, 12283–12291; b) W. Kandioller, C. G. Hartinger, A. A. Nazarov, J. Kasser, R. John, M. A. Jakupec, V. B. Arion, P. J. Dyson, B. K. Keppler, *J. Organomet. Chem.* **2009**, *694*, 922–929; c) W. Kandioller, C. G. Hartinger, A. A. Nazarov, M. L. Kuznetsov, R. O. John, C. Bartel, M. A. Jakupec, V. B. Arion, B. K. Keppler, *Organometallics* **2009**, *28*, 4249–4251; d) M. Hanif, H. Henke, S. M. Meier, S. Martic, M. Labib, W. Kandioller, M. A. Jakupec, V. B. Arion, H. B. Kraatz, B. K. Keppler, C. G. Hartinger, *Inorg. Chem.* **2010**, *49*, 7953–7963; e) M. Hanif, P. Schaaf, W. Kandioller, M. Hejl, M. A. Jakupec, A. Roller, B. K. Keppler, C. G. Hartinger, *Aust. J. Chem.* **2010**, *63*, 1521–1528; f) W. Kandioller, A. Kurzwernhart, M. Hanif, S. M. Meier, H. Henke, B. K. Keppler, C. G. Hartinger, *J. Organomet. Chem.* **2011**, *696*, 999–1010; g) S. M. Meier, M. Hanif, W. Kandioller, B. K. Keppler, C. G. Hartinger, *J. Inorg. Biochem.* **2012**, *108*, 91–95.

[19] R. E. Morris, R. E. Aird, S. Murdoch Pdel, H. Chen, J. Cummings, N. D. Hughes, S. Parsons, A. Parkin, G. Boyd, D. I. Jodrell, P. J. Sadler, *J. Med. Chem.* **2001**, *44*, 3616–3621.
[20] M. A. Bennett, A. K. Smith, *J. Chem. Soc. Dalton Trans.* **1974**, 233–241.
[21] M. R. Pressprich, J. Chambers, *SAINT+Integration Engine*, *Program for Crystal Structure Integration*, Bruker Analytical X-ray systems, Madison, **2004**.
[22] G. M. Sheldrick, *Acta Crystallogr. Sect. A* **2008**, *64*, 112–122.
[23] a) D. R. Robertson, T. A. Stephenson, T. Arthur, *J. Organomet. Chem.* **1978**, *162*, 121–136; b) R. O. Gould, C. L. Jones, D. R. Robertson, T. A. Stephenson, *Cryst. Struct. Commun.* **1978**, *7*, 27–32; c) Y. Hung, W.-J. Kung, H. Taube, *Inorg. Chem.* **1981**, *20*, 457–463; d) W. Weber, P. C. Ford, *Inorg. Chem.* **1986**, *25*, 1088–1092; e) E. A. Ganja, T. B. Rauchfuss, C. L. Stern, *Organometallics* **1991**, *10*, 270–275; f) F. Wang, J. Bella, J. A. Parkinson, P. J. Sadler, *J. Biol. Inorg. Chem.* **2005**, *10*, 147–155; g) S. Grguric-Sipka, I. N. Stepanenko, J. M. Lazic, C. Bartel, M. A. Jakupec, V. B. Arion, B. K. Keppler, *Dalton Trans.* **2009**, 3334–3339.
[24] M. N. Bell, A. J. Blake, M. Schroeder, T. A. Stephenson, *J. Chem. Soc. Chem. Commun.* **1986**, 471–472.
[25] A. F. A. Peacock, M. Melchart, R. J. Deeth, A. Habtemariam, S. Parsons, P. J. Sadler, *Chem. Eur. J.* **2007**, *13*, 2601–2613.
[26] J. P. Williams, J. M. Brown, I. Campuzano, P. J. Sadler, *Chem. Commun.* **2010**, *46*, 5458–5460.
[27] H. Chen, J. A. Parkinson, S. Parsons, R. A. Coxall, R. O. Gould, P. J. Sadler, *J. Am. Chem. Soc.* **2002**, *124*, 3064–3082.
[28] Y. Y. Scaffidi-Domianello, A. A. Legin, M. A. Jakupec, V. B. Arion, V. Y. Kukushkin, M. Galanski, B. K. Keppler, *Inorg. Chem.* **2011**, *50*, 10673–10681.

Received: July 26, 2012
Revised: December 12, 2012
Published online: January 22, 2013

